

Effect of Substrate Temperature on the Physical Properties of Electron Beam Evaporated Cuprous Oxide Thin Films

V. Sravanthi¹, T. Srikanth¹, R. Subba Reddy¹, B.V. Krishna Reddy¹,
A. Sivasankar Reddy^{1*}, P. Sreedhara Reddy², Ch. Seshendra Reddy³

¹Department of Physics, Vikrama Simhapuri University P.G. Centre, Kavali -524201, A.P., India

²Department of Physics, Sri Venkateswara University, Tirupati- 517502, A.P., India

³Department of Materials Science and Engineering, Harbin Institute of Technology, University Town, Shenzhen-518055, China

*Corresponding author email: akepati77@gmail.com

Abstract

In the present work, cuprous oxide (Cu₂O) thin films was prepared on glass substrates using electron beam evaporation and studied the compositional, structural, surface morphology, optical and electrical properties as a function of substrate temperature. The crystallinity of the films increases with substrate temperature and (111) is preferred orientation. The films exhibited smooth surfaces and the RMS roughness of the films decreased from 5.6 to 2.3nm with increasing of the substrate temperature. The films show highest optical transmittance of 79% with optical band gap of 2.2 eV.

Keywords: Cuprous Oxide, Thin Films, Electron beam evaporation, Temperature

1. Introduction

Cuprous oxide(Cu₂O) is an attractive material for wide range of applications such as solar cells [1-2], sensor arrays [3], batteries [4], energy converting devices because of its direct band gap of ~ 2.1eV, high absorption coefficient, natural abundance, non-toxicity [5-8]. Various thin film deposition methods such as magnetron sputtering [9], chemical vapour deposition [10], electro-deposition [11] and electron beam evaporation [12] have been attempted for the deposition of Cu₂O films. Among these techniques, electron beam evaporation (EBE) is an efficient technique for the thin film growth because of material loss is minimal, uniformity of the films over the substrate, useful for depositing alloy and compound materials, films having the stoichiometry close to the bulk. In the present investigation, the Cu₂O films were prepared on the glass substrates and studied the effect of substrate temperature on the physical properties of the films.

2. Experimental

The Cu₂O thin films were deposited on the glass substrates using Cu₂O pellets by electron beam evaporation. The vacuum system is capable of creating an ultimate vacuum of 4x10⁻⁴ Pa. the vacuum chamber was pumped with the combination of diffusion pump and rotary pump. The pressure was measured using a Pirani-Penning gauge combination. The pellet was prepared using high purity (99.99%) Cu₂O powder. The pellets were kept in a water-cooled copper crucible. The thickness of the films was monitored by quartz crystal thickness monitor and the thickness of the films was around ~190 nm. The films deposited at different substrate temperatures from 303 to 573K. The deposition parameters maintained during the preparation of Cu₂O films are given in Table 1.

The crystallographic structure of the films was analyzed by Seifert 3003TT X-ray diffractometer (XRD), using Cu K α radiation ($k = 0.1546\text{nm}$). The microstructure and surface morphology of the films was studied by

scanning electron microscopy (SEM) and atomic force microscopy (AFM), respectively. The chemical composition of the films was analyzed by Energy Dispersive Spectroscopy (EDS) attached with SEM of model Oxford instruments Inca Penta FET X3. Raman spectroscopy was used for determination of chemical bonding configuration in the material. The photoluminescence (PL) spectra were measured with a LS 55 fluorescence spectrometer (Perkin Elmer) at room temperature. The optical transmittance of the films was recorded using a UV–Vis–NIR double beam spectrophotometry. The electrical properties of the films were measured by using standard four-probe method.

Table.1. Deposition parameters of Cu₂O films during deposition

Deposition method	:	electron beam evaporation
Power source	:	e-beam power supply (3kW)
Pellet	:	Cu ₂ O (10mm dia and 3mm thick)
Substrates	:	Glass
Target to substrate distance	:	60 mm
Ultimate pressure (P _U)	:	4x10 ⁻⁴ Pa
Evaporation pressure (P _W)	:	3x10 ⁻² Pa
Substrate temperature (T _S)	:	303, 373, 473 and 573K
Accelerating voltage	:	4 kV
Filament current	:	30 mA
Deposition time	:	8 to 12 min

3. Results and Discussion

The EDS spectra of electron beam evaporated Cu₂O films was shown in Fig.1(a& b) and no reflections of impurity were detected. The films exhibited high oxygen content at substrate temperature of 303K. The films deposited at substrate temperature of 473K were near to the stoichiometry. The obtained composition results at different substrate temperatures were listed in Table 2.

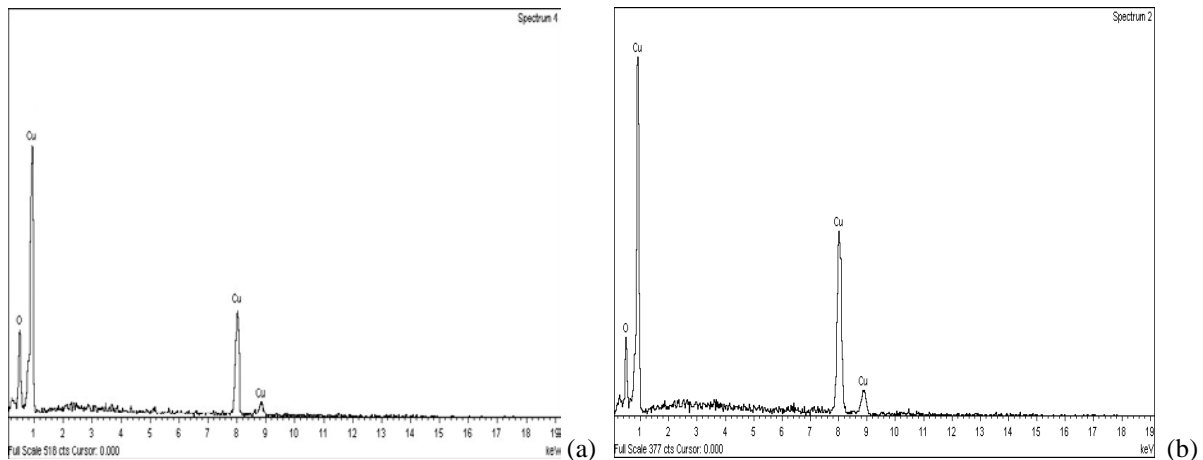


Fig. 1. EDS spectra of Cu₂O films at different substrate temperatures (a) 303 K (b) 473K

Table 2. The compositional results of Cu₂O films by Energy Dispersive Spectroscopy (EDS)

Substrate temperature	Element	Atomic percentage
303K	O K	37.12
	Cu K	62.88
473K	O K	35.39
	Cu K	64.61

3.1 Structural properties

Fig.2. shows the XRD spectra of Cu₂O films deposited at different substrate temperatures. From the XRD results, films exhibited cubic structure and grown preferentially on (111) orientation of Cu₂O. The peak intensity and polycrystalline nature of the films increases with substrate temperature. By increasing the substrate temperature an additional peak of (220) was observed along with (111) orientation. The films exhibited broad peak at 303K was due to insufficient thermal energy and structural defects. The peak position is shifted towards lower angle values with increasing the substrate temperature. The betterment in crystallinity of the films with elevating the substrate temperature was may be due to decrease in defect density[13].

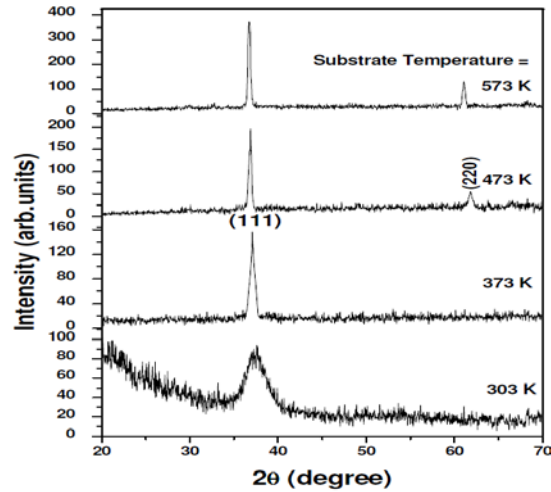


Fig. 2. XRD patterns of Cu₂O films at different substrate temperatures

The average crystallite size of films was calculated by using Scherrer's equation [14], and listed in Table 3. The crystallite size of films was increases more rapidly at higher temperatures. The improvement of the crystallite size with substrate temperature was due to decreasing of the structural defects and improving the crystallinity of the films.

The dislocation density (δ) of the films is defined as the length of dislocation lines per unit volume and was calculated by the following equation [15],

$$\delta = 1/D^2 \quad \text{----- (1)}$$

The dislocation density (δ) of the films decreased with increasing of substrate temperature (Table 3), indicating the reduction of lattice defects and grain boundaries.

The lattice parameter (a) of the films was calculated using the relation

$$d = a / (h^2+k^2+l^2)^{1/2} \quad \text{----- (2)}$$

where h, k and l are the Miller indices. The interplaner spacing (d) was calculated from the X-ray diffraction data using the Bragg's relation. The obtained lattice parameter values are lower than the standard value (ICDD = 4.269Å). The lattice parameter of the films increased with increasing of the substrate temperature (Table 3). In the literature, the decreasing of the lattice parameter of Cu₂O films with increasing of the substrate temperature was reported by Reddy et al. [16].

Table 3. Crystallite size, dislocation density, lattice parameters and RMS roughness values of Cu₂O films at different substrate temperatures

Substrate temperature	Crystallite Size (nm)	Dislocation density (lines/nm ²)	Lattice parameter (Å)	RMS roughness (nm)
303K	5	4.0x10 ⁻²	4.147	5.6
373K	15	4.4x10 ⁻³	4.198	3.9
473K	29	1.2x10 ⁻³	4.226	2.8
573K	35	8.9x10 ⁻⁴	4.237	2.3

3.2 Raman Spectroscopy

Fig.3. shows the Raman spectra of Cu_2O films at different substrate temperature. The films deposited at room temperature exhibited a small peak at 216cm^{-1} corresponds to second order allowed Raman mode of the Cu_2O crystal and no impurity peaks was observed. It indicates that the films deposited at room temperature consist of Cu_2O only. As increasing the substrate temperature the peak at 216cm^{-1} becomes stronger and reduction of full width at half maximum (FWHM), and weak peaks at $150, 248, 516$ and 624cm^{-1} of Cu_2O was appeared. The increasing of the peak intensity and narrowing of the FWHM indicated the improved microstructure with substrate temperature. The obtained Raman results were confirmed the changes observed in XRD results.

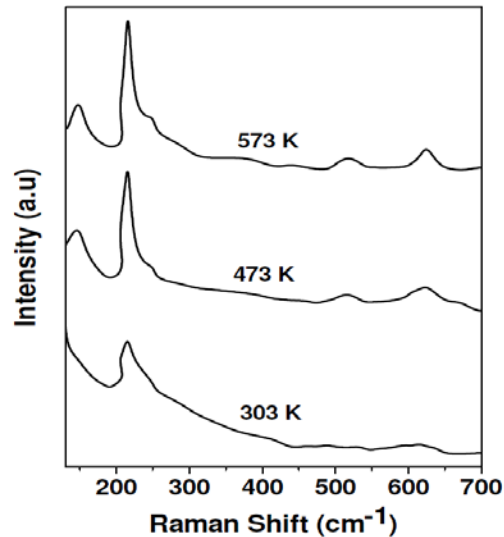


Fig.3. Raman spectra of Cu_2O films at different substrate temperatures

3.3 Microstructure and surface morphology

Fig.4. shows the SEM images of Cu_2O films deposited at different substrate temperatures. The films deposited at 303K exhibited fine grains. The grain size becomes bigger, uniform and smooth surface with increasing the substrate temperature due to agglomeration of smaller grains and decreases of structural defects.

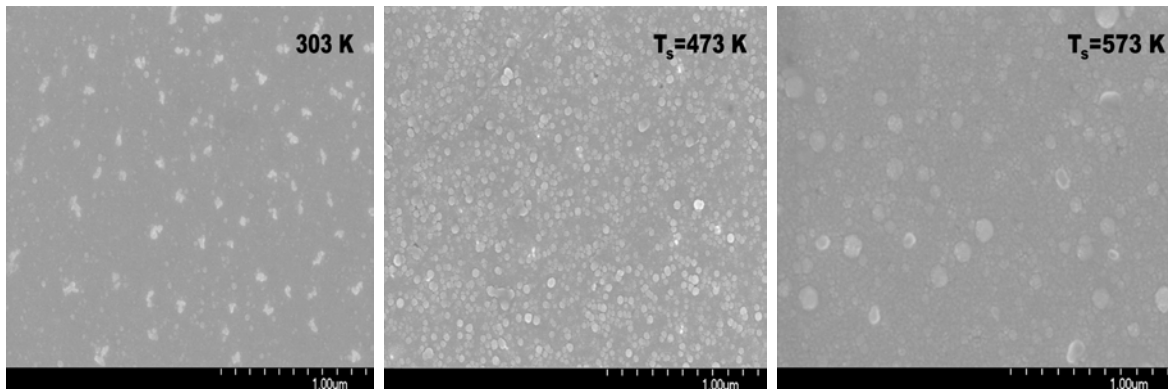


Fig.4. SEM images of Cu_2O films at different substrate temperatures

The surface morphology of films was strongly influenced by the temperature. The three-dimensional AFM images of Cu_2O films deposited at different temperature conditions are shown Fig.5. As seen from the micrographs the films deposited at room temperature exhibited smaller grains with irregular shapes and grain islands. By increasing the substrate temperature the grains grew much bigger and uniformly distributed. The root mean square (RMS) surface roughness of films was measured and listed in Table 3. The roughness of the films decreases gradually with increasing the substrate temperature. This was due to improvement of the crystallinity and reduction of the grain boundaries. The change of surface morphology and RMS roughness of the films with substrate temperature was observed by Hwang et al.[13] and Kumar et al. [17] in magnetron sputtered Cu_2O films.

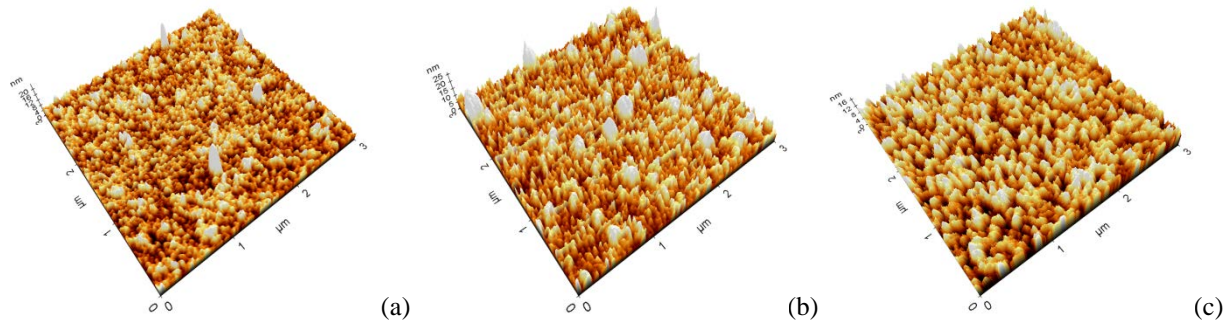


Fig.5. AFM images of Cu₂O films at different substrate temperatures (a) 303K (b) 373K and (c) 473K

3.4 Photoluminescence

The Photoluminescence (PL) spectra of the sample determine that the produced material has enough quality or not [18]. The Photoluminescence (PL) spectra of Cu₂O films at different substrate temperature are shown in Fig.6. The emission peak with weak intensity was located at 500nm (2.48eV) for Cu₂O. The films deposited at substrate temperature of 473K the emission peak intensity increased and an additional peak was observed at 539nm (2.3eV). On further increasing the substrate temperature the peaks intensity was increased and peaks position does not change. The improvement of the emission peak intensity with substrate temperature can be attributed to the decreasing of the structural defects. Johan et al. [19] observed the improvement of the peak intensity with annealing temperature in chemical deposited copper oxide films.

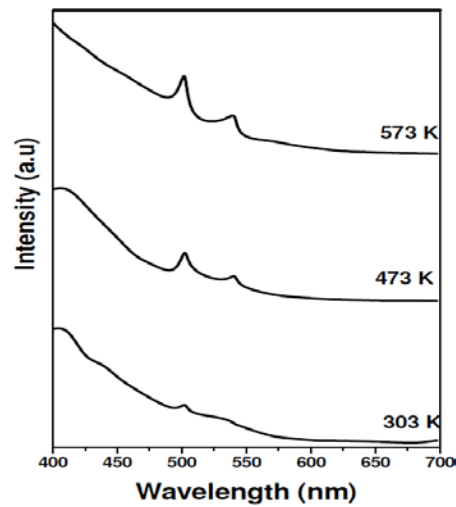
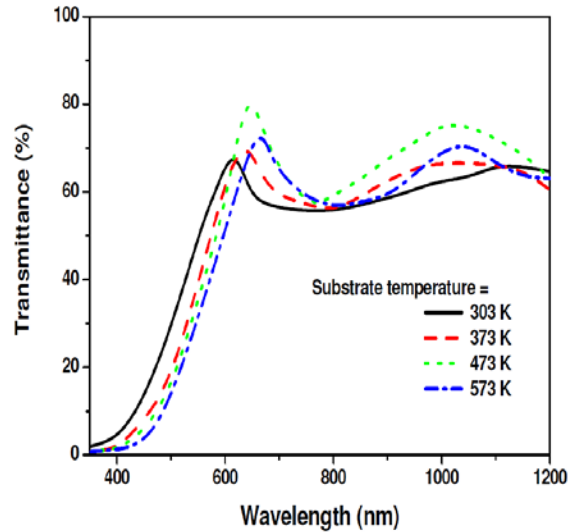


Fig.6. PL spectra of Cu₂O films at different substrate temperatures

3.5 Electrical and Optical properties

The electrical properties of the films are very sensitive to the defects, grain size, strain and surface roughness. The electrical properties of Cu₂O films at different substrate temperatures are listed in Table 4. The resistivity and carrier concentration of the films decreases and mobility increases with increasing of the substrate temperature. The carriers could conduct faster in better crystalline structure consequently mobility increased[20].

It is known that the optical properties are highly influenced by the structural and surface morphology such as density of defects, crystallinity and surface roughness of the films. Fig.7. shows the optical transmittance spectra of Cu₂O films at different substrate temperatures. The optical transmittance of the films increases with increasing substrate temperature from 303K to 473K and decreases at higher temperature of 573K. This was may be due to increasing of the oxygen vacancies at higher temperatures. The absorption edge of the films shifted higher wavelength side with the increase of substrate temperature.


 Fig.7. Optical transmittance spectra of Cu₂O films

The refractive index (n) of the films was calculated using the Swanepoel's envelope method [21] from the transmittance spectra. The refractive index values are increased with increasing the substrate temperature. The obtained values are 2.21, 2.28, 2.35, 2.41 for substrate temperature of 303, 373, 473 and 573K respectively. Wu et al. [22] found that the refractive index of the films decreases with increase of substrate temperature due to enhancement of surface roughness.

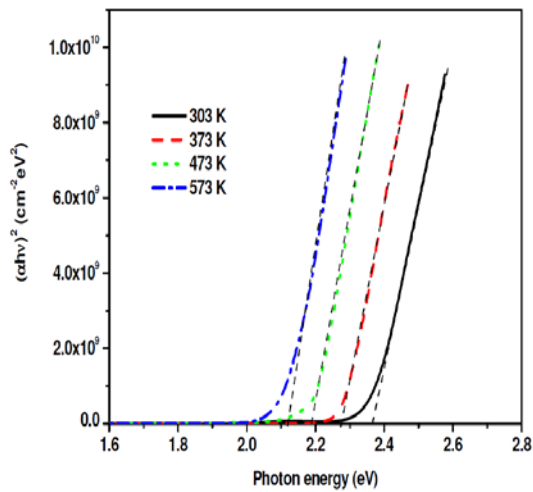

 Fig.8. $(\alpha h\nu)^{1/2}$ versus the photon energy ($h\nu$) of Cu₂O films at different substrate temperatures

Fig.8. shows the variation of the optical band gap values of Cu₂O films as a function of substrate temperature and the obtained values are listed in Table 4. The band gap decreases from 2.37 to 2.14eV with increasing of substrate temperature. The reported band gap values of Cu₂O films in the literature are in the range of 2 to 2.54eV [16, 17-18, 23]. The decreasing of band gap values with increases of temperature is due to reduction of structural defects and enhancement of crystallinity of the films.

 Table 4. Electrical and optical properties of Cu₂O films at different substrate temperatures(T_s)

Substrate temperature	Resistivity (Ωcm)	Hall mobility ($\text{cm}^2/\text{V}\cdot\text{sec}$)	Carrier concentration (cm^{-3})	Transmittance (%) at $\lambda=650$ nm	Band gap (eV)
303K	82	1.8	4.2×10^{16}	61	2.37
373K	56	3	3.7×10^{16}	69	2.28
473K	31	7.2	2.8×10^{16}	79	2.20
573K	20	16	2.0×10^{16}	72	2.14

4. Conclusions

Thin films of Cu_2O have been deposited on glass substrates by electron beam evaporation. From XRD and Raman results, the films exhibited only Cu_2O phase, no impurities such as Cu, CuO was observed. The microstructure and surface morphology of the films improved with temperature. The films deposited at substrate temperature of 473K exhibited highest transmittance of 79% with electrical resistivity of $31\Omega\text{cm}$. The present obtained results make Cu_2O film is a promising candidate p-type semiconductor material for solar cell applications.

References

- [1] D. Barreca, E. Comini, A. Gasparotto, C. Maccato, C. Sada, G. Sberveglieri, E. Tondello, *Sensors Actuators B Chem.* 141 (2009) 270.
- [2] K. Akimoto, S. Ishizuka, M. Yanagita, Y. Nawa, G.K. Paul, T. Sakurai, *Sol. Energy* 80 (2006) 715.
- [3] C.L. Hsu, J.Y. Tsai, T.J. Hsueh, *Sens. Actuators B* 224 (2016) 95.
- [4] F. Hu, K.C. Chan, T.M. Yue, C. Surya, *Thin Solid Films* 550 (2014) 17.
- [5] Z.K. Zheng, B.B. Huang, Z.Y. Wang, M. Guo, X.Y. Qin, X.Y. Zhang, P. Wang, Y. Dai, *J. Phys. Chem. C* 113(2009) 14448.
- [6] H.Y. Xu, J.K. Dong, C. Chen, *Materials Chemistry and Physics* 143(2014) 713.
- [7] S. Sahoo, S. Husale, B. Colwill, T.M. Lu, S. Nayak, P.M. Ajayan, *ACS Nano* 3 (2009) 3925.
- [8] J. Gan, S. Gorantla, H. N. Riise, Ø. S. Fjellva, S. Diplas, O. M. Løvvik, B. G. Svensson, E. V. Monakhov, A. E. Gunnæs, *Applied Physics Letters* 108 (2016) 152110.
- [9] H. Sun, S-C. Chen, C-K. Wen, T-H. Chuang, M.A.P. Yazdi, F. Sanchette, A. Billard, *Ceramics International* 43(2017) 6214.
- [10] S. Eisermann, A. Kronenberger, A. Laufer, J. Bieber, G. Haas, S. Lautenschlager, G. Homm, P.J. Klar, B.K. Meyer, *Phys. Status Solidi A* 209 (2012) 531.
- [11] A. Ashida, S. Sato, T. Yoshimura, N. Fujimura, *J. Crystal Growth*, 468 (2017) 245.
- [12] R. Oommen, U. Rajalakshmi, Sanjeeviraja, *Int. J. Electrochem. Sci.*, 7 (2012) 8288.
- [13] Y. Hwang, H. Ahn, M. Kang, Y. Um, *Current Applied Physics* 15 (2015) S89.
- [14] B.D. Cullity, *Elements of X-ray Diffraction*, second ed., Addison Wesley, London
- [15] H.P. Klug, L.E. Alexander, *X-Ray Diffraction Procedures for Polycrystalline and Amorphous Materials*, Wiley, New York, 1974.
- [16] A. Sivasankar Reddy, P. S. Reddy, S. Uthanna, G. Venkata Rao, A. Klein, *phys. Stat. Sol.(a)* 203(2006) 844.
- [17] B.R. Kumar, B. Hymavathi, T.S. Rao, *Materials Today: Proceedings* 4 (2017) 3903.
- [18] P. B. Ahirrao, S. R. Gosavi, D. R. Patil, M. S. Shinde, R. S. Patil *Arch. Appl. Sci. Res.* 3 (2011) 288.
- [19] M.R. Johan, M.S.M, Suan, N.L. Hawari, H.A. Ching, *Int. J. Electrochem. Sci.* 6 (2011) 6094.
- [20] Y. Ashok Kumar Reddy, A. Sivasankar Reddy, P. Sreedhara Reddy, *J. Mater. Sci. Technol.*, 29 (2013) 647.
- [21] R. Swanepoel *J. Phys. E. Sci. Instrum.* 16 (1983) 1214.
- [22] X. Wu, F. Lai, Y. Lin, Z. Huang, R. Chen, *Proc. SPIE* 6722 (2007) 67222L-1.
- [23] O. Messaoudi, I. Ben assaker, M. Gannouni, A. Souissi, H. Makhoulouf, A. Bardaoui, R. Chtourou, *Applied Surface Science* 366 (2016) 383.